END
DATE
FILMED
12-80
DTIC

MICROCOPY RESOLUTION TEST CHART
NATIONAL BUREAU OF STANDARDS-1963-A

LEVEL II (12)

AD A091112

STUDY OF THE POTENTIAL OF MAIN-BEAM NULLING WITH AN OVERLAPPED-SUBARRAY ANTENNA

Ronald L. Fante

DTIC
S ELECTE
NOV 0 3 1980
E

DDC FILE COPY

ROME AIR DEVELOPMENT CENTER
Air Force Systems Command
Griffiss Air Force Base, New York 13441

80 10 27 090

This report has been reviewed by the RADC Public Affairs Office (PA) and is releasable to the National Technical Information Service (NTIS). At NTIS it will be releasable to the general public, including foreign nations.

RADC-TR-80-117 has been reviewed and is approved for publication.

APPROVED: *Walter Rotman*

WALTER ROTMAN, Chief
Antennas and RF Components Branch
Electromagnetic Sciences Division

APPROVED: *Allan C. Schell*

ALLAN C. SCHELL, Chief
Electromagnetic Sciences Division

FOR THE COMMANDER: *John P. Huss*

JOHN P. HUSS
Acting Chief, Plans Office

If your address has changed or if you wish to be removed from the RADC mailing list, or if the addressee is no longer employed by your organization, please notify RADC (EEA) Hanscom AFB MA 01731. This will assist us in maintaining a current mailing list.

Do not return this copy. Retain or destroy.

REPORT DOCUMENTATION PAGE		READ INSTRUCTIONS BEFORE COMPLETING FORM
1. REPORT NUMBER RADC-TR-80-117	2. GOVT ACCESSION NO. AD-A091 112	3. RECIPIENT'S CATALOG NUMBER
4. TITLE (and Subtitle) STUDY OF THE POTENTIAL OF MAIN-BEAM NULLING WITH AN OVERLAPPED-SUBARRAY ANTENNA		5. TYPE OF REPORT & PERIOD COVERED In-House Report
		6. PERFORMING ORG. REPORT NUMBER
7. AUTHOR(s) Ronald L. Fante		8. CONTRACT OR GRANT NUMBER(s)
9. PERFORMING ORGANIZATION NAME AND ADDRESS Deputy for Electronic Technology (RADC/EEA) Hanscom AFB Massachusetts 01731		10. PROGRAM ELEMENT, PROJECT, TASK AREA & WORK UNIT NUMBERS 61102F 2305J303
11. CONTROLLING OFFICE NAME AND ADDRESS Deputy for Electronic Technology (RADC/EEA) Hanscom AFB Massachusetts 01731		12. REPORT DATE March 1980
		13. NUMBER OF PAGES 22
14. MONITORING AGENCY NAME & ADDRESS(if different from Controlling Office)		15. SECURITY CLASS. (of this report) Unclassified
		15a. DECLASSIFICATION DOWNGRADING SCHEDULE

16. DISTRIBUTION STATEMENT (of this Report)

Approved for public release; distribution unlimited.

17. DISTRIBUTION STATEMENT (of the abstract entered in Block 20, if different from Report)

18. SUPPLEMENTARY NOTES

19. KEY WORDS (Continue on reverse side if necessary and identify by block number)

Antennas
Radiation patterns
Pattern nulls

20. ABSTRACT (Continue on reverse side if necessary and identify by block number)

A study has been made of the possibility of placing nulls in the main beam of an overlapped subarray antenna by controlling the subarray pattern. We have found that it is possible to form main-beam nulls by this technique, but that the nulls are relatively narrow band.
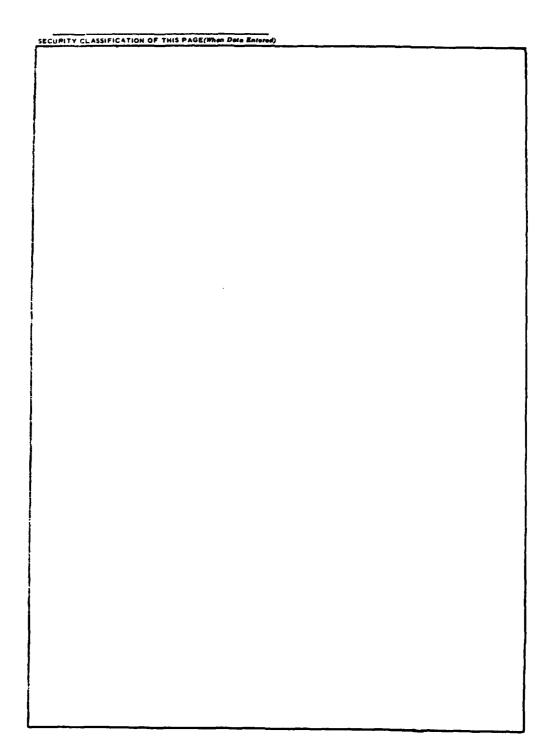
DD 1 JAN 73 1473 EDITION OF 1 NOV 65 IS OBSOLETE

Contents

Illustrations

Study of the Potential of Main-Beam Nulling With an Overlapped-Subarray Antenna

1. INTRODUCTION

In this report we will present the results of our study of the possibility of creating nulls in the radiation pattern of an overlapped subarrayed antenna by placing nulls in the subarray pattern. The overlapped subarray antenna was discussed in detail in Fante[1]; it was shown there that this system has great potential for low-sidelobe wideband scanning. We also briefly discussed the possibility of controlling the subarrays so as to produce pattern nulls. Here we will enlarge upon that discussion.

2. THEORETICAL DISCUSSION

The basic configuration, which is shown in Figure 1, uses a circular lens fed by a hybrid matrix. When an input port (on face A) is excited, a distinct subarray distribution is produced on the output face (plane C) of the lens. Exciting a different port produces a different subarray pattern, which overlaps the first. We can apply different time delays to each subarray simply by applying different time

1. Fante, R.L. (1979) Study of the Radiation Properties of Overlapped Subarrayed Scanning Antennas, RADC-TR-79-293.
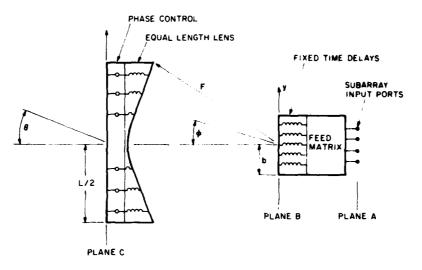
Figure 1. Overlapped Subarrayed Antenna System

delays to each input port. It is this feature which gives the system its large bandwidth.

In Fante[1] is was shown that the radiation pattern F(S) of this system is given by

$$F(S) = C_1 \int_{-1}^{1} d\eta \, a(\eta) \, G[(1 - R) S_o - \gamma R \beta \eta] \cdot \text{sinc} \left[\pi l \gamma R \left(\eta + \frac{RS - S_o}{\gamma R} \right) \right] \tag{1}$$

where $a(\eta)$ is the distribution of the excitation on face B of the feed array; $R = \lambda_o/\lambda$, λ_o is the midband wavelength, λ is the operating wavelength; $l = L/D$, L is the lens width, D is the separation between subarray centers on face C; $S = (D/\lambda_o) \sin \theta$, $S_o = (D/\lambda_o) \sin \theta_o$, θ_o is the scan angle; $\gamma = (bD/\lambda_o F)$, F is the focal length of the main lens, 2b is the width of the feed array (face B); $\beta = 1$ if the feed is a true time-delay system and $\beta = \lambda/\lambda_o$ if the feed is a Butler matrix. Also G(S) is the radiation pattern corresponding to the input distribution on the feed and is defined as

$$G(S) = \sum_{p=-M+1}^{M} \hat{I}_p \, e^{i2\pi(p-1/2)S} \tag{2}$$

where $\hat{I}_p$ is the excitation on the pth input port, and we have assumed 2M input ports.

If the lens were very large ($l \to \infty$) it is readily shown (for β 1) that Eq. (1) reduces to

$$F(S) \simeq G[R(S - S_0)] \; a \left[\frac{RS - S_0}{\gamma R} \right] \qquad (3)$$

so that, in this limit, the system radiation pattern is simply the product of the unsquinted feed pattern $G[R(S - S_0)]$ and the (squinted) distribution on face B of the array.

From Eq. (3) we see that if we could put a null of fractional width δ in the distribution $a(\eta)$ it would appear directly as a null of width ϵ $\gamma\delta$ in the radiation pattern $F(S)$. Consequently we could place nulls in the radiation pattern $F(S)$ by placing nulls in $a(\eta)$. This situation is illustrated graphically in Figure 2, for the case $\lambda = \lambda_0$.
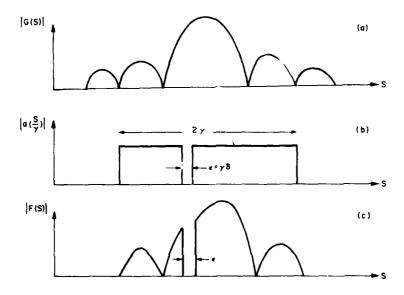

Figure 2. Subarray Nulling for an Infinite Lens ($L \to \infty$)

Unfortunately, in a realistic system the lens width L is finite and the actual radiation pattern is the convolution of Eq. (3) and a sinc function. For example, at midband ($\lambda = \lambda_0$) we can rewrite Eq. (1) as

7

$$F(S) \quad C_2 \int_{-\gamma}^{\gamma} dt \; K(t) \; \text{sinc}[\pi l (t - (S - S_o))] \tag{4}$$

where

$$K(t) \quad a\left(\frac{t}{\gamma}\right) G(t) \tag{5}$$

In writing Eq. (4) we have assumed that $a(-\eta) = a(\eta)$. The physical meaning of Eq. (4) is illustrated in Figure 3. Note that the notch in the radiation pattern in Figure 2c is filled in by finite-lens diffraction effects in Figure 3c. From Figure 3 it is also evident that in order to reproduce the null in $a(\eta)$ in the radiation pattern, we require that the width $2/l$ of the sinc function be less than the null width ε. Consequently a necessary condition for a well-defined null is that

$$\varepsilon l \gg 1 \tag{6a}$$

or equivalently

$$\gamma \delta l \gg 1 \tag{6b}$$

where ε is the null width of the ideal ($l \to \infty$) system in S-space and $\delta/2$ is the fractional portion of face B which is nulled.
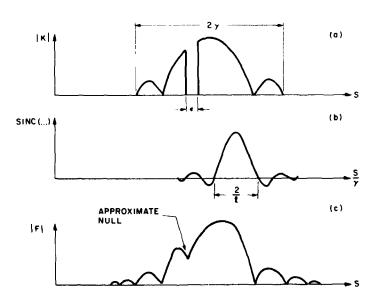

Figure 3. Effect of Subarray Nulling for a Finite Lens

8

3. NUMERICAL RESULTS

In this section we will present computed radiation patterns for some realistic systems. In the last section we treated face B of the feed as a continuum, whereas in reality face B consists of 2N discrete radiators, as shown in Figure 4. We shall assume that these radiators are separated by a distance Δ and have the (complex) excitations $\{a_n\}$ for $-N + 1 \leq n \leq N$. In all cases studied in this report we shall also assume that $2M = 16$, so that there are 16 overlapped subarrays across the lens. Finally we have defined $\gamma_o = \Delta D / \lambda_o F$.
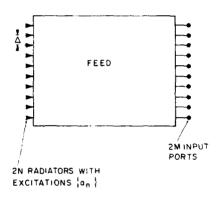

Figure 4. Magnified Version of the Feed

We shall first study the effect of simply setting several of the $\{a_n\}$ equal to zero while keeping all the others equal to unity. In Figure 5 we show the result at midband for $2N = 32$ when we attempt to place a null at $S - S_o = -0.02$ by setting $a_o = a_1 = a_2 = 0$, but keeping a_{-15} through a_{-1} and a_3 through a_{16} equal to unity, for the case when $\ell = 16.4$ (so that the lens is slightly larger than the width of the 16 overlapped subarrays). We note that the desired null actually splits into two distinct deep nulls (depth greater than -70 dB) with a -38 dB hump in the middle, so that there is no true notch. There are two other important points to note. The gain at $S - S_o = 0$ (where in a real radar system the target would be located) is reduced by -25 dB and the system sidelobes have been increased by approximately 13 dB. Consequently, for a lens with $\ell = 16.4$ it does not make too much sense to attempt to place nulls too close to the center of the main beam.

In Figure 6 we show what happens when we move the null further from the center of the main beam (to $S - S_o = -0.035$). In this case the gain at $S - S_o = 0$ is reduced by only 7 dB and the sidelobes increased by only 8 dB, relative to the
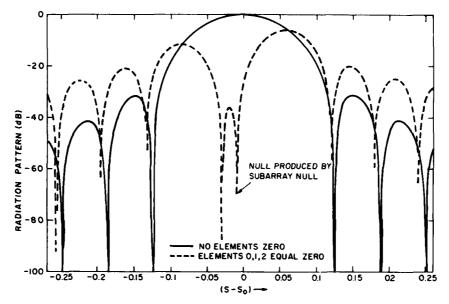
9

Figure 5. Effect of Attempting to Place a Null at S - S_0 ~ -0.02 by Setting
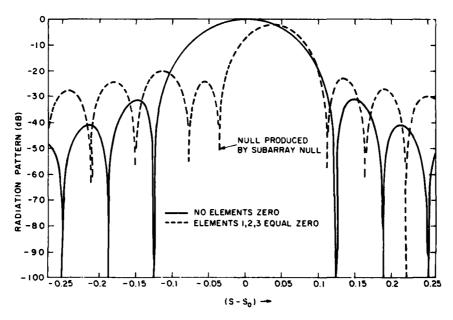Elements 0, 1, and 2 on Face B Equal to Zero

Figure 6. Effect of Attempting to Place a Null at S - S_0 = -0.035 by Set-
ting Elements 1, 2, and 3 on Face B Equal to Zero

10

case when there is no main-beam null. When the null is moved further out to $S - S_o = -0.06$ the gain at $S - S_o = 0$ is only -2 dB and there is then a 6-dB increase in the sidelobe levels, as is evident from Figure 7. As the null is moved to still further positions from the center of the main beam there is essentially no gain loss at $S - S_o = 0$, nor any increase in the sidelobe levels, as we can see from Figures 8 and 9.

One point clearly evident from Figures 6 to 9 is that the null is very narrow and is consequently narrow band.[*] One would expect that the null region could be broadened by increasing the lens size l because then the radiation pattern would be a more faithful reproduction of $K = aG$, as we see from Figure 3. In Figure 10 we compare the null at $S - S_o = -0.06$ for the case when $l = 16.4$ with that for $l = 32$. For $l = 32$ the null begins to approximate a notch, but with a -28 dB hump in the middle. The magnitude of this hump is decreased as l is increased. For $l = 40$, the hump maximum has been lowered to -38 dB, and for $l = 50$ the hump maximum is -48 dB. Consequently, for large enough l the pattern begins to exhibit a true notch.

Unfortunately, making $l = L/D$ large is not a very practical solution for obtaining a null with a large instantaneous bandwidth, because it requires making the lens much wider than the region occupied by the illumination from the 16 overlapped subarrays. This means that the lens needs many extra phase shifters without a corresponding decrease in beamwidth. This situation is shown pictorially in Figure 11.

We have also studied methods for moving the position of the null. This is readily achieved by controlling the element excitations on face B of the feed. This is illustrated by the results in Figure 12. For example, a null at $S - S_o = -0.0745$ can be obtained by setting $a_3 = 0.9$, $a_4 = a_5 = a_6 = a_7 = 0$, $a_8 = 0.1$ and all the other a_n equal to unity. This null can be moved to $S - S_o = -0.0735$ by setting $a_3 = 0.8$, $a_4 = a_5 = a_6 = a_7 = 0$, $a_8 = 0.2$ and all other a_n equal to unity. We can also compensate for changes in operating frequency by varying the $\{a_n\}$. In Figure 13 we show what happens to a main-beam null as the frequency is changed but all $\{a_n\}$ are kept constant. We note that a 1 percent frequency change results in a considerable null displacement. Thus, the pattern gain in the direction of a jammer at $S - S_o = -0.06$ would be -60 dB at $f = f_o$ (midband) but would be only -18 dB at $f = 1.01 f_o$. However, as can be seen from Figure 14 it is possible to change the excitations $\{a_n\}$ so as to keep the null in the same direction at two different frequencies. Thus, although the null has only a 0.3 percent instantaneous

---

[*]For example, the fractional bandwidth for a -40-dB null is of order W/S_o where W is the -40-dB null width. From Figures 7 to 9 we see that $W \simeq 0.003$ so that for large scan angles ($S_o \simeq 1.5$) the fractional bandwidth is of order of 0.2 percent.
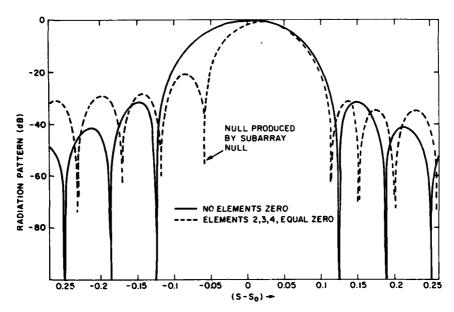
Figure 7. Effect of Attempting to Place a Null at S - S$_o$ = -0.06 by Setting Elements 2, 3, and 4 on Face B Equal to Zero
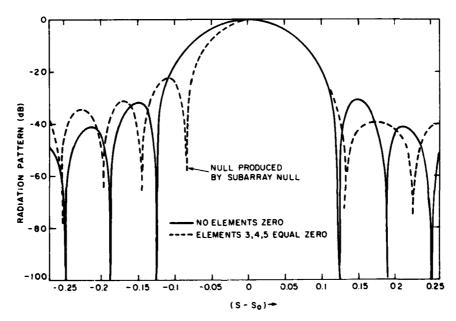

Figure 8. Effect of Attempting to Place a Null at S - S$_o$ = -0.085 by Setting Elements 3, 4, and 5 on Face B Equal to Zero
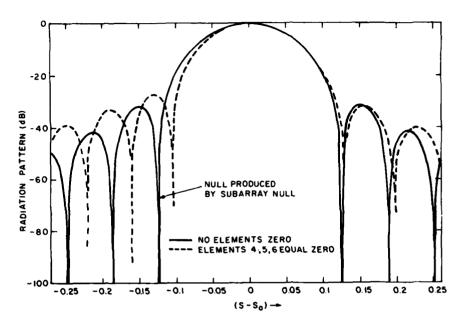
12

Figure 9. Effect of Attempting to Place a Null at S - S$_o$ = -0.105 by Setting Elements 4, 5 and 6 on Face B Equal to Zero
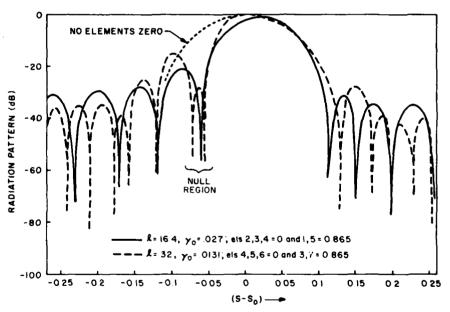

Figure 10. Effect of Increasing Lens Size ℓ in Order to Broaden the Null at S - S$_o$ = -0.06
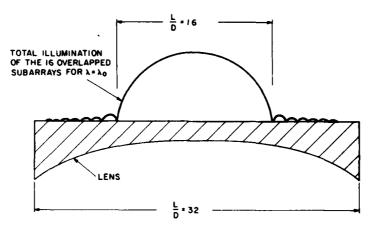
13

Figure 11. Illustration of the Illumination on the Lens When
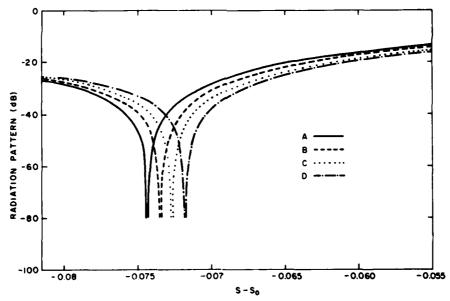$l = L/D$ is Much Larger than the Number of Subarrays (2M)

Figure 12. Use of Element Excitations to Control Null Placement for
$l = 16.4$, $\gamma_0 = 0.0135$, $R = 1$, $2N = 64$, $2M = 16$ and Elements 4
Through 7 on Face B Equal to Zero. Also: A) $a_3 = 0.9$, $a_8 = 0.1$,
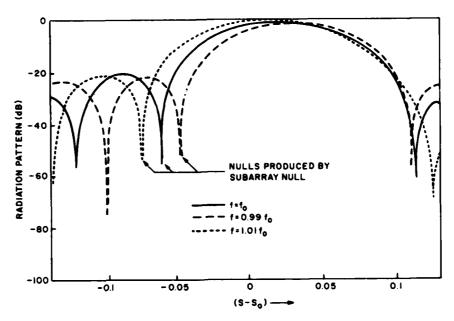B) $a_3 = 0.8$, $a_8 = 0.2$, C) $a_3 = 0.7$, $a_8 = 0.3$, D) $a_3 = 0.6$, $a_8 = 0.4$

14

Figure 13. Effect of Varying Frequency on the Null Position When l = 16.4, γ_O = 0.027, 2M = 16, 2N = 32, S_O = 1.5, and Elements 2, 3, and 4 on Face B are Equal to Zero
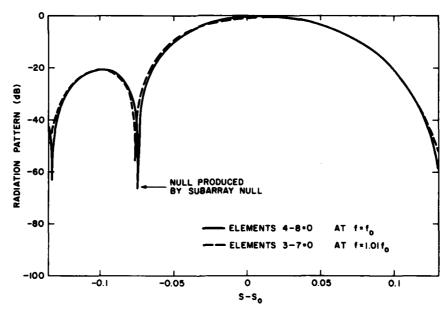

Figure 14. Use of Element Switching to Maintain a Null at the Same Position as the Frequency Is Changed, for the Case When l = 16.4, γ_O = 0.0135, 2N = 64, 2M = 16, and S_O = 1.5

15

bandwidth, it can have a much broader bandwidth when used in a frequency-hopping system since we can program the excitation coefficients $\{a_n\}$ so that they are switched to a new set $\{a_n'\}$ each time the frequency hops to a new value.

An alternate approach to ameliorate the deleterious effects of a jammer has been suggested by Mailloux.[2] In his technique one does not attempt to place a single null (or notch) at the jammer location, but rather null-out nearly one entire half of the beam. This concept is illustrated in Figure 15, for the ideal case of an infinite lens ($L \to \infty$). Such a system is inherently wideband, as we can see from the pictorial representations in Figure 16, for three frequencies $f = f_0$, $f = f_0 + \Delta f$ and $f = f_0 - \Delta f$. Unfortunately in a realistic system, in which the lens width L is finite, we cannot duplicate the behavior shown in Figure 15. In Figure 17 we show the radiation pattern at midband when one half of the elements on face B are set equal to zero (that is, we set a_1 through a_{16} equal to zero and a_{-15} through a_0 equal to unity). We note that, because of finite-lens effects the radiation pattern is not zero for $S - S_0 < 0$, although it is below what would be present if no elements were set equal to zero. In addition, the gain loss at $S - S_0 = 0$ (target location) is nearly 5 dB and the sidelobe levels are increased by approximately 10 dB (relative to the case when no elements are nulled). We might expect to make the pattern for $S - S_0 < 0$ a better approximation to the ideal pattern (see Figure 15) by tapering the distribution of the a_n's as shown in Figure 18. The effect of this taper is shown in Figure 19. We note that the taper improves the pattern for $S - S_0 < 0$ only slightly, but does produce a noticeable lowering of the sidelobe levels. Furthermore, we do not get any significant further improvement in the pattern by tapering both sides of the $\{a_n\}$ distribution as shown in Figure 20.

Clearly, the approximation of the realistic pattern to the ideal one becomes better as $l = L/D$ is increased. In Figures 21 and 22 we show the patterns for the case when $l = 32$. In Figure 21 we have used the taper $\exp(-0.25\, n^2)$ on the $\{a_n\}$ for $n \geq 0$ and the results in Figure 22 correspond to a taper $\exp(-0.125\, n^2)$ for $n \geq 0$ with all other $a_n = 1$. We note that the taper $\exp(-0.125\, n^2)$ gives quite reasonable results (we also tried numerous other tapers but $\exp(-0.125\, n^2)$ was about the best). In fact we can see how much improvement there is over the case when $l = 16.4$ by comparing the results for $l = 16.4$ with those for $l = 32$. This is done in Figure 23. We note that for $l = 32$ the pattern is below -40 dB for all $S - S_0 \leq -0.06$, and this is very much better than the results for $l = 16.4$.

There is, of course, one major flaw in increasing lens size to improve the approximation to the ideal; since we are making the lens large, why not use the whole lens and not just part of it in the first place? This would give a pattern only half as wide in $S - S_0$ space so that jammers inside the main beam would be

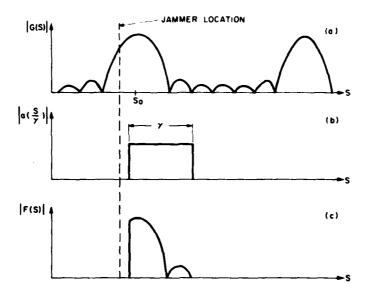2. Mailloux, R.J. (1980) private communication.

16

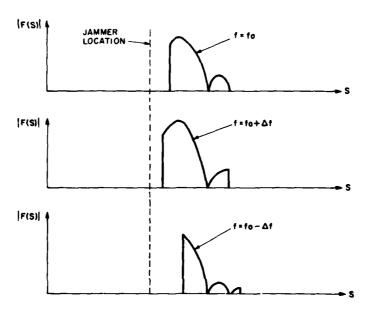Figure 15. Effect of Setting Nearly One Half of the Subarray Pattern Equal to Zero (for L → ∞)

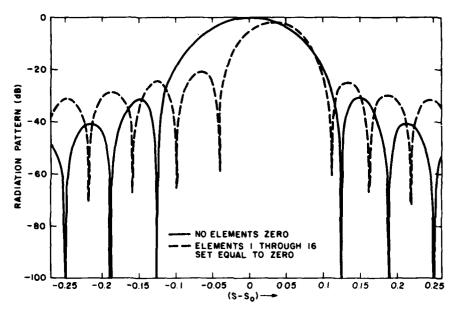Figure 16. Effect of Changing Frequency on the Ideal System Depicted in Figure 15

17

Figure 17. Effect on the Radiation Pattern Setting Half of the Elements on Face B Equal to Zero, for the Case When $l = 16.4$, $\gamma_0 = 0.027$, $2M = 16$, $2N = 32$, and $R = 1$
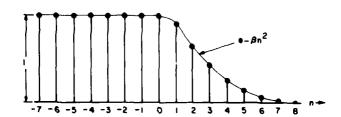

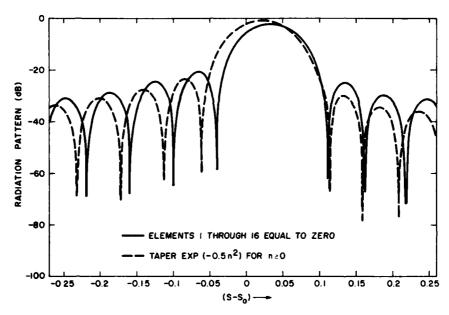
Figure 18. Values of a_n vs n for the Case When $2N = 16$

18

Figure 19. Effect of a Taper on Face B on the Radiation Pattern for the
Case When $l = 16.4$, $\gamma_o = 0.027$, $2M = 16$, $2N = 32$, and $R = 1$
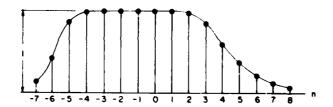
Figure 20. Typical Case When the Distribution of the a_n
Is Tapered at Both Ends
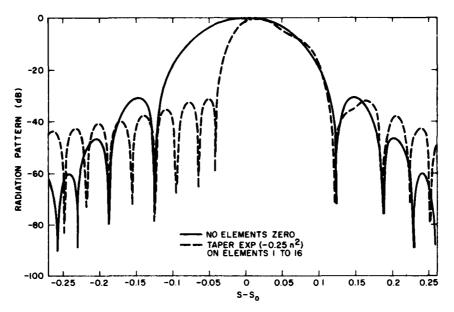
Figure 21. Effect on the Radiation Pattern of Placing a Taper exp $(-0.25 n^2)$ on Elements 1 Through 16 on Face B, Assuming $l = 32$, R 1, 2N = 32, 2M = 16, and γ_0 0.0131
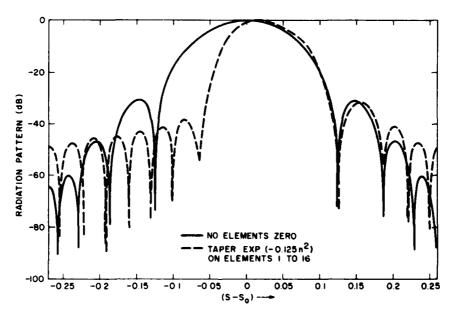
Figure 22. Effect on the Radiation Pattern of Placing a Taper exp $(-0.125 n^2)$ on Elements 1 Through 16 on Face B, Assuming $l = 32$, R 1, 2N 32, 2M 16, and γ_0 0.0131
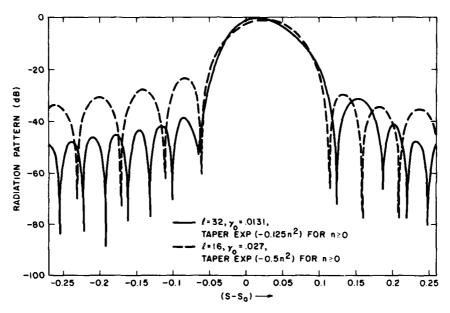
20

Figure 23. Effect of Lens Size on the Radiation Pattern of a System in Which One Half of the Elements on Face B Are Tapered

outside the narrowed beam corresponding to the lens twice as wide. Thus, this scheme gives wide bandwidth, but at the expense of a large lens. It is essentially the same problem we ran into earlier when attempting to place a notch in the main beam.

4. CONCLUSIONS

We have studied the possibility of placing nulls in the main beam of the over-lapped subarrayed antenna by controlling the excitation of the elements on face B of the feed in Figure 1. We have found that it is possible to place a null in the main beam by setting the excitation on several of the elements on face B equal to zero, but that such nulls are extremely narrow band (about 0.3 percent instantan-eous bandwidth) under normal conditions. We have found that it is possible to produce wideband nulls with this method but at the expense of increasing the lens size (while keeping the number of subarrays constant) relative to the subarray spacing (l large). We have also studied the possibility of tapering half the ele-ments on face B towards zero so as to produce an entire null region over half of the main beam. This method is somewhat successful but in order to get deep wideband nulls we again are forced to make l large.

21

We have not studied the possibility of null control by controlling the excitations at both face A and face B as shown in Figure 24, but this is an intriguing possibility. Perhaps with control at both faces, a null of wider bandwidth can be produced.
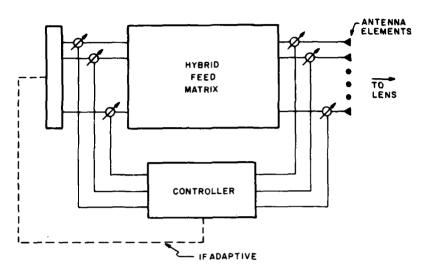

Figure 24. Control of Excitations at Both Input and Output Ports

22

MISSION
of
Rome Air Development Center

RADC plans and executes research, development, test and selected acquisition programs in support of Command, Control Communications and Intelligence (C^3I) activities. Technical and engineering support within areas of technical competence is provided to ESD Program Offices (POs) and other ESD elements. The principal technical mission areas are communications, electromagnetic guidance and control, surveillance of ground and aerospace objects, intelligence data collection and handling, information system technology, ionospheric propagation, solid state sciences, microwave physics and electronic reliability, maintainability and compatibility.